Quantum Mechanics II Final Project: Graphene and Dirac Equations

Christopher McBride, Junghyun Min[1]

[1]*Department of Physics and Astronomy, The Johns Hopkins University, Baltimore, MD 21218, USA*

In this paper, we explore the quantum-electronic properties of graphene, introduce the quantum mechanical foundation which describes graphene, study the electronic band structure of graphene to derive and discuss its "massless Dirac Fermion."

I. BACKGROUND AND MOTIVATION

A. Graphene

In 2010, Andre Geim and Konstantin Novoselov (Figure 1) won the Nobel Prize in Physics for their research on graphene, or as they call it, the flatland [5]. They have successfully produced, isolated, identified, and characterized this two dimensional crystalline material, a single atomic layer of carbon. Graphene has interesting and unique properties [6]. Its electronic properties produces an unusual quantum Hall effect [1], is a transparent conductor, suggests implications in particle physics involving an exotic type of tunneling. It is also mechanically interesting, with much more strength than steel, stiffer than diamond, and has the greatest elasticity of any crystal. It thermally and electrically conducts, and so can function as a flexible conductor [6].

Graphene is particularly exciting as a material because it is a two-dimensional material. A suspended sheet of pure graphene consists of a planar layer of carbon atoms bonded in a honeycomb lattice [3]. Carbon atoms can form many different structures other than graphene; this includes graphite, carbon nanotubes, and fullerenes (the Bucky Ball being a well known example). Geim and Novoselov, as part of their Nobel prize winning research, successfully produced the two-dimensional structure known as graphene. As a result of its structure, graphene was suspected to have a particularly interesting electronic band structure, which we will study in section II A.

FIG. 1: Andre Geim and Konstantin Novoselov, winners of 2010 Nobel Prize in Physics

B. Dirac Equation

Paul Dirac derived his relativistic wave equation (known as the Dirac Equation) in 1928. The description of special relativity in quantum mechanics had some interesting implications, including the existence of antimatter, and further applications in quantum field theory [8]. The standard derivation for the relativistic correction of quantum mechanics begins by describing the Hamiltonian eigen-equation as

$$\hat{H}|\Psi\rangle = E|\Psi\rangle = \sqrt{c^2p^2 + m^2c^4}|\Psi\rangle \tag{1}$$

It is interesting to see how, from this equation, and the relations $\hat{H} = -i\hbar\frac{d}{dt}$, and $\hat{p} = -i\hbar\nabla$, we may get the Klein-Gordon equation

$$(\frac{1}{c^2}\frac{d^2}{dt^2} - \nabla^2 + \frac{m^2c^2}{\hbar^2})|\Psi\rangle = 0 \tag{2}$$

Under a different formulation we may demand that $\hat{H}|\Psi\rangle = \hat{K}|\Psi\rangle$, where $\hat{K}^2 = c^2\hat{p}^2 + m^2c^4$. In this way we may define a relation such that

$$\hat{K} = c\vec{\alpha}\cdot\hat{\vec{p}} + \beta mc^2 \tag{3}$$

From this it is easy to see that the elements $\vec{\alpha}$ and β can not be complex numbers, for this would require either $\vec{\alpha}$ or β to be zero, which won't give us a satisfying solution. Therefore we treat $\vec{\alpha}$ and β as matrices. Continuing with the derivation we get

$$\begin{aligned}\hat{K}^2 &= [c\sum_i \alpha_i p_i + \beta mc^2][c\sum_j \alpha_j p_j + \beta mc^2] \\ &= \frac{c^2}{2}\sum_i\sum_j(\alpha_i\alpha_j + \alpha_j\alpha_i)p_i p_j + \beta^2 m^2 c^4 + ...\end{aligned} \tag{4}$$

This formulation requires that

$$\beta^2 = 1$$
$$\alpha_i\beta + \beta\alpha_j = 0$$
$$\alpha_i\alpha_j + \alpha_j\alpha_i = 2\delta_{ij}$$

which, as you can see, are several anti-commutation relations defining the structure of our relativistically corrected kinetic energy. References to these relations generally use the term Dirac Algebra or Clifford Algebra [7]. Now, given that $\hat{H}$ is a Hermitian operator, for our system to be consistent, $\vec{\alpha}$ and β must also be Hermitian operators. This places the constraint on our matrices that they must have even dimensions (easily verified by seeing that the trace of α_i and β must equal zero). This leaves us the job of finding satisfying matrix descriptions. If we begin by attempting to find matrices of dimension 2x2 we recover the Pauli-Spin matrices. These satisfy Dirac Algebra, but are not sufficient for our purposes. Instead we look to 4x4 matrices which results in the matrix formulation shown in figure 2 where γ^0 is β, and γ^1, γ^2, and γ^3 are the three matrices for $\vec{\alpha}$. We are now equipped to state fully the Dirac Equation

$$(c\sum_{i=1}^{3}\alpha_i p_i + \beta mc^2)|\Psi(x,t)\rangle = i\hbar\frac{\delta}{\delta t}|\Psi(x,t)\rangle \tag{5}$$

For our purposes we will be using the Dirac Equation to discuss electrons in graphene. The Dirac Equation in matrix form appears in figure 3.

II. MAIN RESULTS

We will first follow Leggett's lecture to derive massless Dirac fermions from graphene, in section II A and then discuss it in section II B.

$$\gamma^0 = \begin{pmatrix} 1 & 0 & 0 & 0 \\ 0 & 1 & 0 & 0 \\ 0 & 0 & -1 & 0 \\ 0 & 0 & 0 & -1 \end{pmatrix}, \qquad \gamma^1 = \begin{pmatrix} 0 & 0 & 0 & 1 \\ 0 & 0 & 1 & 0 \\ 0 & -1 & 0 & 0 \\ -1 & 0 & 0 & 0 \end{pmatrix}$$

$$\gamma^2 = \begin{pmatrix} 0 & 0 & 0 & -i \\ 0 & 0 & i & 0 \\ 0 & i & 0 & 0 \\ -i & 0 & 0 & 0 \end{pmatrix}, \qquad \gamma^3 = \begin{pmatrix} 0 & 0 & 1 & 0 \\ 0 & 0 & 0 & -1 \\ -1 & 0 & 0 & 0 \\ 0 & 1 & 0 & 0 \end{pmatrix}.$$

FIG. 2: The Dirac Matrices, also know as gamma matrices.

$$\begin{pmatrix} i\frac{\partial}{\partial t} - m & 0 & i\frac{\partial}{\partial z} & i\frac{\partial}{\partial x} + \frac{\partial}{\partial y} \\ 0 & i\frac{\partial}{\partial t} - m & i\frac{\partial}{\partial x} - \frac{\partial}{\partial y} & -i\frac{\partial}{\partial z} \\ -i\frac{\partial}{\partial z} & -i\frac{\partial}{\partial x} - \frac{\partial}{\partial y} & -i\frac{\partial}{\partial t} - m & 0 \\ -i\frac{\partial}{\partial x} + \frac{\partial}{\partial y} & i\frac{\partial}{\partial z} & 0 & -i\frac{\partial}{\partial t} - m \end{pmatrix} \begin{pmatrix} \psi^1 \\ \psi^2 \\ \psi^3 \\ \psi^4 \end{pmatrix} = \begin{pmatrix} 0 \\ 0 \\ 0 \\ 0 \end{pmatrix}$$

FIG. 3: Fully expanded matrix form of the Dirac Equation.

A. Electronic Band Structure of Graphene

Here, we first consider a perfectly flat and isolated sheet of graphene, as shown in figure 4. In graphene, carbon atoms, whose electronic structure is $(1s)^2(2s)^2(2p)^4$, hybridize to form three sp^2 orbitals, and arrange themselves in a planar, honeycomb lattice form, forming 120° angles.

Note here that the structure includes two inequivalent sublattices, labeled A and B in figure 4, which are mirror images of one another. It is convenient to choose lattice vectors $\boldsymbol{a_1}$ and $\boldsymbol{a_2}$, also shown in figure 4, as

$$\boldsymbol{a_1} = \frac{a}{2}(3, \sqrt{3}), \qquad \boldsymbol{a_2} = \frac{a}{2}(3, -\sqrt{3}) \tag{6}$$

where a corresponds to the closest C-C spacing, ($\approx 1.42\mathring{A}$). Then, the reciprocal lattice vectors $\boldsymbol{b_1}$ and $\boldsymbol{b_2}$ which is given by $\boldsymbol{a_i} \cdot \boldsymbol{b_j} = 2\pi\delta_{ij}$ are

$$\boldsymbol{b_1} = \frac{2\pi}{3a}(1, \sqrt{3}), \qquad \boldsymbol{b_2} = \frac{2\pi}{3a}(1, -\sqrt{3}). \tag{7}$$

Next, we define the first Brillouin zone (FBZ) of the reciprocal lattice, as bounded by planes

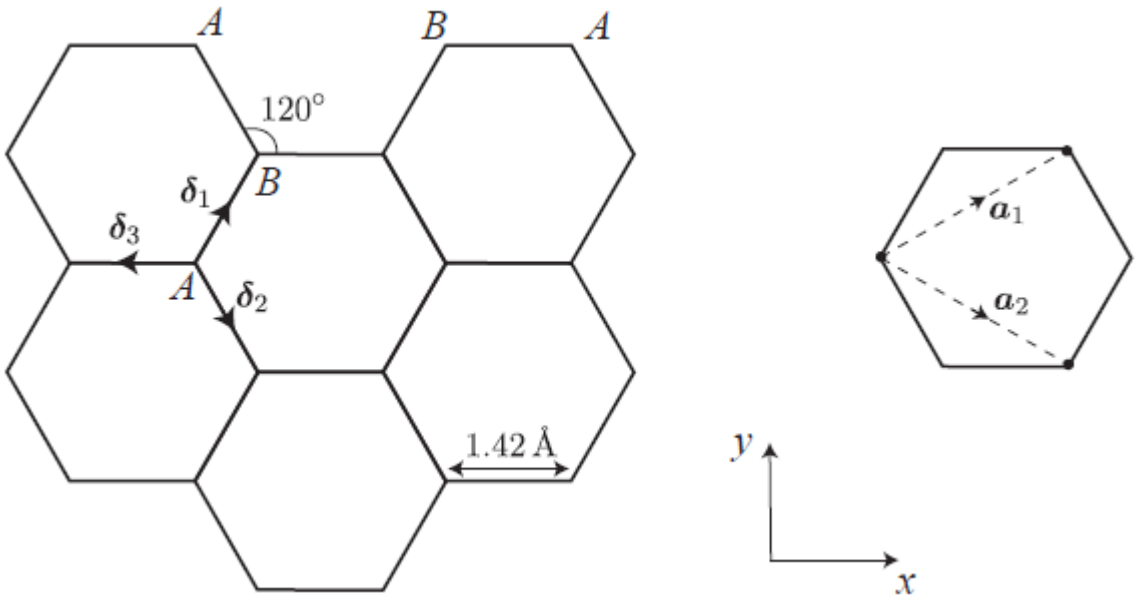

FIG. 4: Isolated flat graphene and its primitive lattice vectors [3].

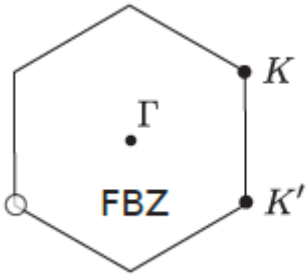

FIG. 5: A first Brillouin zone of the reciprocal lattice, with two equivalent corners K and K' [3].

bisecting the vectors to the nearest reciprocal lattice points. With this, we have a FBZ in the form of the original hexagons of the honeycomb lattice rotated by $\pi/2$, as shown in 5. The six corners are three sets of two equivalents, so without loss of generality we only consider two equivalent corners, K and K', whose momentum-space positions are given by

$$\boldsymbol{K} = \frac{2\pi}{3a}(1, \frac{1}{\sqrt{3}}), \qquad \boldsymbol{K'} = \frac{2\pi}{3a}(1, -\frac{1}{\sqrt{3}}). \tag{8}$$

In addition, we note here that the three nearest-neighbor vectors in position space for sublattice A, denoted $\boldsymbol{\delta_1}$, $\boldsymbol{\delta_2}$, and $\boldsymbol{\delta_4}$, and shown in figure 4, are given by

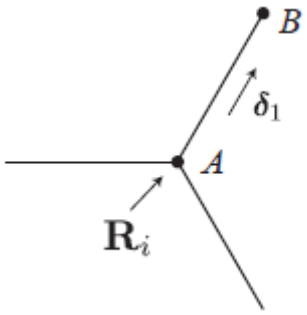

FIG. 6: Visualization of positions used in equation 11 [3].

$$\boldsymbol{\delta_1} = \frac{a}{2}(1, \sqrt{3}), \quad \boldsymbol{\delta_2} = \frac{a}{2}(1, -\sqrt{3}), \quad \boldsymbol{\delta_3} = -a(1, 0) \tag{9}$$

while the vectors are given with opposite signs for sublattice B.

We first model the electronic band structure, with nearest-neighbor hopping only, with tight-binding Hamiltonian

$$\hat{H}_{TB,n.n.} = -t \sum_{ij=n.n.} (a^\dagger_{i\sigma} b_{j\sigma} + H.c.) \tag{10}$$

and TB eigenfunctions of form

$$\begin{bmatrix} \alpha_k \\ \beta_k \end{bmatrix} = \sum_i \exp i\boldsymbol{k} \cdot \boldsymbol{R_i^0} \begin{bmatrix} a_i^\dagger e^{-i\boldsymbol{k}\cdot\boldsymbol{\delta_1}/2} \\ b_i^\dagger e^{i\boldsymbol{k}\cdot\boldsymbol{\delta_1}/2} \end{bmatrix}, \tag{11}$$

where $\boldsymbol{R}_i^0$ is a reference point, arbitrarily chosen to be at A, B separated from A by $\boldsymbol{\delta}_1$, and $b_i^\dagger$ creates an electron on the B atom on cell i, illustrated in figure 6.

Now, the resulting Hamiltonian is purely off-diagonal in the **k**-representation:

$$\hat{H}_k = \begin{bmatrix} 0 & \Delta_k \\ \Delta_k^* & 0 \end{bmatrix}, \quad \Delta_k \equiv -t \sum_{l=1}^{3} \exp i\boldsymbol{k} \cdot \boldsymbol{\delta_l}, \tag{12}$$

and combining with the nearest-neighbor vectors in equation 9, we get explicitly

$$\Delta_k = -texp - ik_x a(1 + 2\exp(i\frac{3k_x a}{2})cos\frac{\sqrt{3}}{2}k_y a) \tag{13}$$

and eigenvalues of the Hamiltonian is $\epsilon_k = \pm|\Delta_k|$.

Here, we consider if there are values of $\boldsymbol{k}$ for which $\Delta_k = 0$ (or equivalently, $\epsilon_k = 0$):

$$\begin{aligned} &\frac{3k_x a}{2} = 2n\pi, \qquad cos\frac{\sqrt{3}}{2}k_y a = -1/2 \quad (n = 0, \pm 1, \pm 2, ...) \\ \text{or} \quad &\frac{3k_x a}{2} = (2n+1)\pi, \qquad cos\frac{\sqrt{3}}{2}k_y a = 1/2. \end{aligned} \tag{14}$$

The second set of equations are satisfied at the equivalent corner points K and K', as described in figure 5. They are called "Dirac points". One takeaway point from this is that given the symmetry of energy band about the point $\epsilon_k = 0$, and that this condition is satisfied at two Dirac point, as opposed to a metal, whose complete surface of **k**-values meet the condition. Thus, for exactly half filling of the band, the density of states at the Fermi level is exactly zero. Also, in the absence of doping graphene has exactly one electron per spin per atom, so taking spin into account, the band is exactly half filled. Thus, undoped graphene is a perfect semimetal!

Now, we discuss energy spectrum and eigenfunctions for **k** close to a Dirac point. Without loss of generality, we can pick the point $\boldsymbol{K}$. First we define $\boldsymbol{q} = \boldsymbol{k} - \boldsymbol{K}$, and expanding the expression for $\boldsymbol{\Delta_k}$ around **q**=0, we have

$$\Delta(\boldsymbol{q}) - \simeq 2te^{iK_x a}\boldsymbol{q}\cdot\boldsymbol{\nabla_k}(e^{3ik_x a/2}cos\frac{\sqrt{3}}{2}k_y a)_{\boldsymbol{k}=\boldsymbol{K}} = -\frac{3ta}{2}(\exp - iK_x a)(iq_x - q_y). \tag{15}$$

Extracting an overall constant factor $-i\exp - iK_x a$, we get

$$\Delta((q)) = \hbar v_F(q_x - iq_y)(1 + \mathcal{O}(q/K)^2), \qquad v_F \equiv 3ta/2\hbar \cong 10^6 m/sec. \tag{16}$$

Now, it is suggestive to write the Hamiltonian in the following way:

$$\hat{H} = \hbar v_F \begin{bmatrix} 0 & q_x + iq_y \\ q_x - iq_y & 0 \end{bmatrix} \equiv \hbar v_F \hat{\boldsymbol{\sigma}}\cdot\boldsymbol{q}, \qquad \epsilon(q) = \pm v_F|q|, \tag{17}$$

where $\hat{\boldsymbol{\sigma}}$ is an operator whose components are Pauli matrices. Formally speaking, Hamiltonian 17 represents a massless particle of spin 1/2, such as the neutrino, with c replaced with Fermi velocity v_F. Thus, graphene produces an analog to particle physics in a solid-state context, as anticipated in section I A [3].

B. Graphene and Massless Dirac Fermions

Touched on briefly in section II A, we may consider how massless Dirac fermions emerge from the graphene structure. A full description is aptly given by Jean-Noel Fuchs in his work on Dirac fermions [9]. Essentially, within the honeycomb lattice each carbon shares a σ bond with its neighbors, leaving a single conduction electron. It is because of this electron that a Hilbert space may be constructed (from the carbon $2p_z$ orbitals). The Hamiltonian in sublattice subspace emerges as a 2-dimensional Dirac Hamiltonian. In the Weyl representation this Hamiltonian appears as

$$H_D^{\pm} = v_F(\pm\alpha_x p_x + \alpha_y p_y) \tag{18}$$

where v_F is the Fermi velocity ($\approx c/300$).

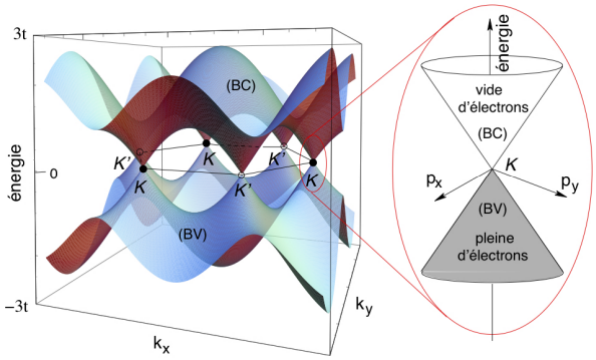

FIG. 7: Shows the tight-binding band structure of graphene with an overlay showing fermion energy. The zoomed picture shows the linear dispersion of massless Dirac fermions. Credit: Fuchs, J. [9]

.

C. Remaining questions

· What is the first Brillouin zone and what is its significance?

· What does it mean that for exactly half filling of the band the density of states at the Fermi level is exactly zero?

· What is graphene doping?

D. Further Thoughts and Future of Graphene

One of the most compelling aspects of graphene is how it might be applied in materials engineering. The unique quantum mechanical nature of graphene not only makes it a fascinating structure to work with theoretically and experimentally but also in its applications to technology. It seems likely that the the rapid magneto-transport property of graphene would lead to some interesting applications in electronic devices. Even when not considering the quantum-electric properties, its' mechanical uses due its light weight, its flexibility, and durability makes it ideal for use in a new generation of practical every day technologies.

In addition, as graphene was "hidden" as fullerenes and nanotubes [3], there may be countless possibilities in manipulating flat graphene into different shapes for different purposes, especially with its flexibility and durability.

Its relevance to the field of physics will likely extend through several decades as its deeper nature is probed, and is adapted to explore more complex systems that are difficult to describe theoretically. Put in another way, solutions to the Dirac equation may not always be found in a sufficiently complex system, but experimental results may still be applicable when physicists may compare and contrast the properties between graphene and the more complex extension of that system.

---

[1] K. S. Novoselov, Z. Jiang, Y. Zhang, S. V. Monosov, H. L. Stormer, U. Zeitler, J. C. Maan, G. S. Boebinger, P. Kim, and A. K. Geim, *Room-temperature quantum hall effect in graphene*, Science **315**, 1379 (2007).

[2] A. H. Neto, F. Guinea, N. M. R. Peres, K. S. Novoselov, and A. K. Geim, *The electronic properties of graphene*, Reviews of Modern Physics, **81**, 110-162 (2009).

[3] A. J. Leggett, *Graphene: Electronic band structure and Dirac fermions*, University of Illinois at Urbana-Champagne, 1-12 (2010).

[4] G. W. Semenoff, *Condensed-matter simulation of a three-dimensional anomaly*, Phys. Rev. Lett. **53**, 26, 2449-245 (1984).

[5] K. S. Novoselov, *Graphene: materials in the flatland*, the University of Manchester, 1-31 (2010).

[6] Class for Physics, *Graphene: scientific background on the Nobel Prize in Physics 2010*, the

Royal Swedish Academy of Sciences, 1-11 (2010).

[7] Martin, Victoria. *The Dirac Equation and Spinors*. The University of Edinburgh, 4 Feb. 2012, www2.ph.ed.ac.uk/~vjm/Lectures/SHParticlePhysics2012_files/PPNotes2.pdf#page=2.

[8] P.W. Atkins (1974). *Quanta: A handbook of concepts*. Oxford University Press. p. 52. ISBN 0-19-855493-1.

[9] Fuchs, J (June 4, 2013). *Dirac fermions in graphene and analogues: magnetic field and topological properties*. Sec 1.2. https://arxiv.org/pdf/1306.0380.pdf.